

## Pathways to a clean $\gamma$ ( $\phi_3$ ): From B to Super B-factories

David Atwood

*Dept. of Physics and Astronomy, Iowa State University, Ames, IA 50011*

Amarjit Soni

*Theory Group, Brookhaven National Laboratory, Upton, NY 11973*

(Dated: November 2, 2018)

The implementation of various methods for the determination of  $\gamma$  through direct CP violation arising in the interference of  $b \rightarrow c$  and  $b \rightarrow u$  processes in charged as well as neutral  $B$  meson decays are considered. We show that the inclusion of  $D^0$  resulting from  $D^{*0} \rightarrow D^0 + \pi^0(\gamma)$  say via  $B \rightarrow KD^{*0}$  makes a significant difference in the attainable accuracy for  $\gamma$ . Both exclusive and inclusive decays of the  $B^\pm$  and  $B^0$  to states containing  $D^0/\bar{D}^0$  followed by both inclusive and exclusive decays of the  $D^0$  are discussed. It is shown that with statistics which might be obtained at  $B$  factories ( $5 - 10 \times 10^8$  B-pairs) a  $1\sigma$  determination of  $\gamma$  to  $\approx \pm 5^\circ$  may be possible depending on the efficiency of reconstruction, backgrounds and the details of the decay amplitudes involved. The role of data from a charm factory as well as effects of  $D^0$  mixing are discussed. Extraction of  $\gamma$  with accuracy that is roughly commensurate with the intrinsic theory error of these methods (i.e. around 0.1%), which is an important goal, will require  $> 10^{10}$  B-pairs, namely a Super-B Factory.

PACS numbers: 12.15.Hh; 11.30.Er; 13.25.Hw

### I. INTRODUCTION

The B factories at KEK and SLAC have made remarkable progress in many areas of B-physics, in particular in the extraction of Cabibbo Kobayashi Maskawa (CKM) [1] parameters crucial to testing the standard model. Indeed, the determination of  $\sin 2\beta$  via  $B \rightarrow J/\psi K_S$  in such a way that there is no dependence on theoretical assumptions promises to usher in a new era of precision tests of the CKM paradigm[2, 3].

The determination of the other two unitarity angles,  $\alpha$  and  $\gamma$ , without theoretical errors still presents a considerable experimental challenge. The corresponding CP violating effects are somewhat harder to observe in channels sensitive to  $\alpha$  and  $\gamma$ . In addition, effects sensitive to  $\alpha$  such as  $B \rightarrow \pi\pi$  are subject to some electroweak penguin contamination.

In this paper, we will consider the application of several related methods for determining the angle  $\gamma$  through the decay  $B^- \rightarrow K^- D^0$  [4, 5, 6, 7]. The key idea of these methods is that the decay  $B^- \rightarrow K^- D^0$  and  $B^- \rightarrow K^- \bar{D}^0$  can interfere if the  $D^0$  decays to a common hadronic final state as shown in the generic Feynman diagram Fig. 1 where, as an example, of a CP-non-eigenstate (CPNES) case, the mode  $B^- \rightarrow K^- [\mathbf{D}^0 \rightarrow K^+ \pi^-]$  is shown (here we use  $\mathbf{D}$  to indicate a superposition of  $D^0$  and  $\bar{D}^0$ ). Similarly for the case of CP-eigenstate (CPES) [4] an example would be  $D^0, \bar{D}^0 \rightarrow K_S \omega$ , say. These interferences involves the weak phase  $\gamma$  together with unknown strong phases from the  $B$  and  $D$  decays. A minimum of two modes that are common to the decays of  $D^0, \bar{D}^0$  are needed to solve for the weak phase  $\gamma$ , along with the two strong phases and the suppressed  $\text{Br}(B^- \rightarrow K^- \bar{D}^0)$  that appears to be very difficult to measure experimentally because of serious backgrounds [5].

There are a number of variations of this process which we will consider here. We will show that an effective method for the determination of  $\gamma$  is to allow the  $K$  or the  $D$  to assume vector or pseudo-scalar forms. Thus the generic reaction has four variations  $B^- \rightarrow K^- \mathbf{D}^0$ ,  $B^- \rightarrow K^{*-} \mathbf{D}^0$ ,  $B^- \rightarrow K^- \mathbf{D}^{*0}$ , and  $B^- \rightarrow K^{*-} \mathbf{D}^{*0}$ . In principle, this set of reactions could be further generalized to higher excited states of  $D$  or  $K$  but we will not further consider this case here. Unless the production of such higher states is surprisingly large, the four reactions listed are likely to be of the greatest experimental interest.

In the cases involving  $\mathbf{D}^{*0}$  the  $\mathbf{D}^{*0}$  decays to a  $\mathbf{D}^0$  with  $\pi^0$  or  $\gamma$  and then the  $\mathbf{D}^0$  decays to the hadronic final state common to  $D^0$  and  $\bar{D}^0$ . One complication that arises in the case of  $B^- \rightarrow K^{*-} \mathbf{D}^{*0}$  is that there are three helicity amplitudes which can, in principle, be separated by considering angular correlations between the decays. Here, however, we will just consider the inclusive data, that is without attempting to perform the angular analysis such as that considered in [8].

We will also briefly consider the neutral  $B$  decays of the same form such as  $B^0 \rightarrow K^{*0} \mathbf{D}^0$ . Here we will only consider the self tagging [9, 10] cases, where the flavor of the  $B$  is determined by having a charged  $K$  in the final state, for instance  $B^0 \rightarrow [K^{*0} \rightarrow K^+ \pi^0] \mathbf{D}^0$ . For non-self-tagging modes such as  $B^0 \rightarrow K_S \mathbf{D}^0$  one must also take into

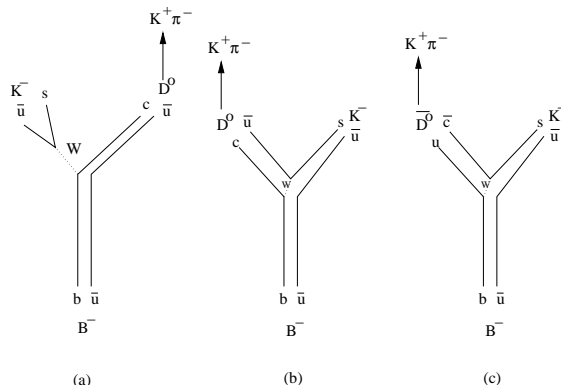


FIG. 1: Feynman diagrams for  $B^- \rightarrow K^- [\mathbf{D}^0 \rightarrow K^+ \pi^-]$ . Diagrams (a) and (b) are  $b \rightarrow c$  transitions where  $\mathbf{D}^0 = D^0$  while (c) is the  $b \rightarrow u$  transition with  $\mathbf{D}^0 = \bar{D}^0$ . Diagram (a) is color allowed while (b) and (c) are color suppressed;  $\bar{D}^0 \rightarrow K^+ \pi^-$  is Cabibbo allowed, whereas  $D^0 \rightarrow K^+ \pi^-$  is doubly Cabibbo suppressed.

account the oscillation of the  $B^0$  in which case the main dependence of the results is on  $\delta \equiv \beta - \alpha + \pi \equiv 2\beta + \gamma$  as considered in [11, 12, 13, 14, 15].

The key feature of these decays which allows the determination of  $\gamma$  is the possibility of interference between  $D^0$  and  $\bar{D}^0$  channels. This can be accomplished by the selection of the common hadronic final state of the  $\mathbf{D}^0$  decay. The formalism given in the appendix shows how to calculate the total rate for both inclusive and exclusive decays of the  $D^0$ . In this case we refer to a decay which is controlled by a single quantum amplitude as exclusive, for instance decays to 2 pseudoscalars or a pseudoscalar and a vector would fall into this category. Decays which are the incoherent sum of many amplitudes are inclusive. This would include decays to two vectors where no measurement of the polarization is made; multibody decays where the data is integrated over all or part of phase space or states which consist of several decay modes of different particle content. In the formalism of the appendix, in such cases we introduce an additional parameter  $R$  which quantifies the degree of coherence[7] associated with the amplitudes composing the inclusive decay. This parameter, along with the average strong phase, must also be determined from the data.

The same methodology can also be applied to inclusive decays of the parent  $B$ , for instance,  $B^- \rightarrow K^- \mathbf{D}^0 + X$  or the case  $B^- \rightarrow K^{*-} D^{*0}$  (summed over polarization). Since this approach makes no assumption concerning the structure of the amplitude of such inclusive decays it therefore introduces no potential model dependence into the analysis. In contrast, the approach of [16] assumes a resonance structure but, with this modest assumption concerning the amplitude, is able to extract more observables since the phase space dependence is fit in detail; they explicitly treat the case of  $B^- \rightarrow K^- \pi^0 \mathbf{D}^0$ , where the  $\mathbf{D}^0$  decays to a CP eigenstate.

The decays of the  $D^0$  can be further categorized according the quark level transition involved, it may either be Cabibbo allowed (CA), for instance  $D^0 \rightarrow K^- \pi^+$ ; singly Cabibbo suppressed (SCS), for instance  $D^0 \rightarrow K^{*+} K^-$ [17] or Doubly Cabibbo suppressed (DCS) such as  $D^0 \rightarrow K^+ \pi^-$ . Note that if  $D^0 \rightarrow X$  is DCS then  $\bar{D}^0 \rightarrow X$  is CA while if  $D^0 \rightarrow X$  is SCS then so is  $\bar{D}^0 \rightarrow X$ . In addition, some two body decays such as  $D^0 \rightarrow \pi^+ \pi^-$ ,  $D^0 \rightarrow K^+ K^-$  and  $D^0 \rightarrow K_S \pi^0$  are CP eigenstates (CPES). The bulk of these are of the form  $K_{S,L} + X$ ; since they are CA and in particular about 5% of the branching ratio is to negative CPES (CPES-) of the form  $K_S + X$  [18].

Section II discusses some of the B and D decays that are of interest. In there we also spell out, in some detail, our working assumptions. In section III we discuss the expectation for the size of the CP asymmetry in various modes. Section IV illustrates extraction of  $\gamma$  for some of the combination of data sets. In section V we re-visit the feasibility of flavor tagging of  $D^0$  versus  $\bar{D}^0$  using their semi-leptonic decays. Section VI deals with  $D\bar{D}$  mixing effects. In section VII we briefly discuss the use of neutral (rather than charged) B-mesons, in conjunction with their self-tagging modes and direct CP violation to get  $\gamma$ . Multibody B decays are briefly discussed in section VIII. In section IX we briefly mention how these determinations of  $\gamma$  may play out at a super-B factory and we close with a briefly summary in section X. Some details on the formalism are relegated to the appendix.

## II. B AND D DECAY MODES

In this paper, we will compare the results of various determinations of  $\gamma$  by carrying out  $\chi^2$  scans assuming a certain level of input data.

The actual number of events observed at a given integrated luminosity will therefore depend on phases and often even on branching ratios which are unknown. To quantify the statistical error, we will assume that a specific fixed

| Initial $B$ decay         | Subsequent $D^0$ decay | Number of events |
|---------------------------|------------------------|------------------|
| $B^- \rightarrow K^- D^0$ | $K^+ \pi^-$            | 25               |
| $B^- \rightarrow K^- D^0$ | $K^{*+} \pi^-$         | 14               |
| $B^- \rightarrow K^- D^0$ | $K^+ \pi^- + n\pi$     | 106              |
| $B^- \rightarrow K^- D^0$ | $CPES-$                | 827              |

TABLE I: Initial “core data sample” used where the number of events is assumed to be distributed among the given mode and its charge conjugate. The corresponding number of events for the three other initial  $B^-$  decays:  $D^{*0}K^-$ ,  $D^0K^{*-}$  and  $D^{*0}K^{*-}$  are assumed to be the same.

number of events of each type are seen. This will have the side effect of implying a slight variation in  $\hat{N}_B$ , (the number of  $B$  mesons) $\times$ (acceptance) with the input parameters which will generally lie within a reasonable range. There are two advantages of adopting this approach: first of all, the  $\chi^2$  values determined for a given combination of modes will be less dependent on the underlying unknown parameters and secondly, the sample calculations should give an idea of the precision which can be reached given the quota of events indicated.

In order to make contact with actual experimental conditions, we will use a simple model for the acceptance of various modes. For each observable particle  $x$  in the final state we will assign a relative acceptance  $R_x$ . In addition we will assume there is overall reduction in acceptance of  $R_{cut}$  due to the relatively hard acceptance cuts which would be required to find the signals suggested in these methods. Following the discussion in [16, 19], the particular values we will use in our numerical estimates are:

$$\begin{aligned}
 R_{\pi^\pm} = 0.95 \quad R_{K^\pm} = 0.8 \quad R_{\pi^0} = 0.5 \quad R_\gamma = 0.5 \quad R_{\eta \rightarrow 2\gamma} = 0.5 \\
 R_{cut} = \frac{1}{6} - \frac{1}{3}
 \end{aligned} \tag{1}$$

Perhaps the most striking initial manifestation of CP violation in this system will be the case where  $B^- \rightarrow K^- D^0$  and the  $D^0$  subsequently decays to  $K^+ \pi^-$ . As pointed out in [5] the large decay rate  $B^- \rightarrow K^- D^0$  coupled with the Doubly Cabibbo Suppressed (DCS) decay  $D^0 \rightarrow K^+ \pi^-$  gives about the same amplitude as the color-suppressed decay  $B^- \rightarrow K^- \bar{D}^0$  coupled with the Cabibbo Allowed (CA) decay  $\bar{D}^0 \rightarrow K^+ \pi^-$ . The result is that the CP violation in this combination is potentially large. In addition, this final state is relatively easy to reconstruct so it will likely provide the earliest evidence of CP violation from the interference of  $b \rightarrow u$  and  $b \rightarrow c$  transitions.

In this paper, for simplicity, we will assume a core data sample of 100  $D^0 \rightarrow K^+ \pi^-$  events of this sort which are distributed equally among four possible parent decays ( $B^- \rightarrow \mathbf{D}^0 K^-$ ,  $B^- \rightarrow \mathbf{D}^{*0} K^-$ ,  $B^- \rightarrow \mathbf{D}^0 K^{*-}$  and  $B^- \rightarrow \mathbf{D}^{*0} K^{*-}$ ). In particular we will assume an initial data sample as shown in Table I. Note that in each case the number of events is distributed between the given mode and its charge conjugate.

In order to estimate what this implies concerning the value of  $\hat{N}_B$ , let us assume that the interference between the two channels of  $B^- \rightarrow K^- [\mathbf{D}^0 \rightarrow K^+ \pi^-]$  is zero; indeed this should be true on average. In Table V discussed below, we list the branching ratios which we use for various  $B$  and  $D$  decays. Using these numbers, the sum of the two channels neglecting interference is  $26 \times 10^{-8}$ . Since only charged  $B$ 's are being used here, for the needed 25  $K \pi$  events, it will require  $N_\gamma = (3 - 6) \times 10^8$ , where we have included  $R_{cut} = [\frac{1}{6} - \frac{1}{3}]$ ; corresponding to 300-600  $fb^{-1}$ . To estimate the number of events for the other modes we will combine the above acceptances for each of the final state particles.

We will assume that the product of these two quantities is roughly the same between the different combinations of  $K^*$  and  $D^{*0}$  in order to give the same number of events in each case, the other modes tend to have larger branching ratios but will likely have smaller acceptances.

The  $K^+ \pi^-$  mode alone given in Table I is not sufficient to determine  $\gamma$ , in general at least one additional decay mode of  $D^0$  is required. Another prominent DCS mode which could be used is  $K^{*+} \pi^-$  [5, 6]. In principle, this is a 3 body mode and can interfere to some extent with other quasi 2 body modes; however, the  $K^*$  is sufficiently narrow that taking it as a two body mode should be a good approximation.

In the CA channel, this mode is about 1.5 times that of  $D^0 \rightarrow K^- \pi^+$  and we will assume that this is roughly true for the overall  $B^- \rightarrow K^- [\mathbf{D}^0 \rightarrow K^{*+} \pi^-]$ . The  $K^{*+}$  has three dominant decay modes, each of which has branching ratio  $\sim \frac{1}{3}$ :  $K_L \pi^+$ ,  $K_S \pi^+$  and  $K^+ \pi^0$ . In the case of  $K_L \pi^+$  the  $K_L$  will be hard to detect and we will assume that the acceptance is negligible. For  $K_S \pi^+$  the  $K_S$  decays  $\frac{2}{3}$  to  $\pi^+ \pi^-$  giving a final state which is likely to have high acceptance. There is, however a background from the CA decay  $D^0 \rightarrow \pi^+ [K^{*-} \rightarrow K_S \pi^-]$  so that some cuts may be needed. We will assume that this channel has an acceptance reduced by  $\frac{1}{2}$  due to the cuts giving a total of  $\frac{1}{3}$  taking

| CP Eigenstate   | Br [%] | Est. Acceptance | eff. Br [%] |
|---|--------|-----------------|-------------|
| $K_S\pi^0$  | 1.14   | 0.360           | 0.410       |
| $K_S[\eta \rightarrow \pi^+\pi^-\pi^0; \pi^+\pi^-\gamma]$ | 0.38   | 0.231           | 0.088       |
| $K_S\rho^0$   | 0.73   | 0.648           | 0.473       |
| $K_S[\omega \rightarrow 3\pi]$                            | 1.1    | 0.324           | 0.356       |
| $K_S[\eta' \rightarrow \pi^+\pi^-\gamma; \pi^+\pi^-\eta]$ | 0.93   | 0.188           | 0.175       |
| $K_S[\phi \rightarrow K^+K^-]$                            | 0.47   | 0.261           | 0.123       |
| Total CPES-   | 4.75   |                 | 1.625       |
| $K_S[f_2(1270) \rightarrow \pi^+\pi^-]$                   | 0.22   | 0.549           | 0.121       |
| $\pi^+\pi^-$  | 0.14   | 0.648           | 0.091       |
| $K^+K^-$  | 0.412  | 0.512           | 0.211       |
| $K_S K_S$   | 0.03   | 0.567           | 0.017       |
| Total CPES+   | 0.58   | 0.55            | 0.319       |

TABLE II: This table consists of a list of some of the CPES decays of the  $D^0$ . For each mode, the branching ratio (Br) is given as the central value in [18] and the acceptance estimated as discussed in the text. The effective branching ratio is the product of these two.

into account  $Br(K_S \rightarrow \pi^+\pi^-)$ . There is no such problem with  $K^{*+} \rightarrow K^+\pi^0$  but the neutral pion in the final state will reduce the acceptance by 0.5.

Overall then, the acceptance for  $B^- \rightarrow K^-[\mathbf{D}^0 \rightarrow K^{*+}\pi^-]$  is 0.22. The total number of events then should be .55 times the case of  $\mathbf{D}^0 \rightarrow K^+\pi^-$  so we will assume 14 events for each  $D^{(*)0}K^{(*)-}$  combination as shown in Table I.

Another class of modes are CP eigenstates (CPES) as considered in [4] which we will refer to as GLW modes. Such modes, excluding those with  $K_L$  have a branching ratio of about 5%.

In Table II we list some such modes with the central value of the branching ratio from [18] and acceptance for  $B^- \rightarrow K^-[D^0 \rightarrow CPES]$  estimated as above. The product of these two gives an effective branching ratio; for CP=-1 (CPES-) states it is 1.6% while for CP=+1 (CPES+) this is .32%. In our estimates we will consider the CPES- states only in which case if there are 25  $K^+\pi^-$  events there should be about 827 CPES- events as indicated in Table I.

Singly Cabibbo suppressed modes which are not CP eigenstates such as  $D^0 \rightarrow K^{*+}K^-$  have been considered in [17]. These have the property that the decay of  $D^0$  to the charge conjugate i.e.  $D^0 \rightarrow K^+K^{*-}$  will also be possible. We will therefore be able to observe four different reactions:

$$\begin{aligned}
B^- &\rightarrow K^-[\mathbf{D}^0 \rightarrow K^{*+}K^-] \\
B^+ &\rightarrow K^+[\mathbf{D}^0 \rightarrow K^{*-}K^+] \\
B^- &\rightarrow K^-[\mathbf{D}^0 \rightarrow K^{*-}K^+] \\
B^+ &\rightarrow K^+[\mathbf{D}^0 \rightarrow K^{*+}K^-]
\end{aligned} \tag{2}$$

Note that the strong phase difference in the first two decays is the opposite of that in the second two. In fact, both of these modes taken together will allow the determination of  $\gamma$ . The central values of the two  $D$  branching ratios [18] are 0.38% for  $D^0 \rightarrow K^{*+}K^-$  and 0.22% for  $D^0 \rightarrow K^{*-}K^+$ . Estimating the number of such events in our data sample as above we find about 50 in each case.

Another data set which might be obtained is by using semi-leptonic (SL) decays of the  $D^0$  to directly monitor the  $b \rightarrow u$  transition  $B^- \rightarrow K^{(*)-}\bar{D}^{(*)0}$ . This is likely to be difficult as discussed in [5] as it requires flavor tagging of  $D^0$  versus  $\bar{D}^0$  which has non-trivial backgrounds from semi-leptonic decays of the  $B$ . In Section V, we will discuss some possible strategies for overcoming this potential difficulty. To illustrate possible usefulness of this determination, we will then show the effect on  $\gamma$  extraction assuming that data of this sort gives a 1- $\sigma$  error on  $Br(B^- \rightarrow K^-D^0)$  ranging from 200% to 10%. Thus the implementation of the original GLW[4] method to obtain  $\gamma$ , may be envisioned with the use of CPES along with flavor tagging through the use of SL data.

Additional information to reconstruct  $\gamma$  may also be obtained through the use of a  $\psi(3770)$  charm factory to measure the strong phases in  $D^0$  decays [7, 20, 21, 22]. As discussed in [7] this can provide additional information so that  $\gamma$  can also be determined through inclusive modes. Even if charm factory data is not available, if we combine inclusive modes with other exclusive modes, there is enough information to determine  $\gamma$  and we shall explore a number of such possibilities below.

In particular, as an example of such a mode we will consider the combination of modes  $K^+\pi^- + n\pi$ . Most likely each of these modes will be detected separately so additional information [6, 23] may be obtained by separating such

| CP Eigenstate                 | Br [%] (CA) | Est. Acceptance | eff. Br [%] |
|-------------------------------|-------------|-----------------|-------------|
| $K^- \pi^0 \pi^+$             | 11.1        | .304            | 3.37        |
| $K^- \pi^+ \pi^+ \pi^-$       | 7.5         | .549            | 4.12        |
| $K^- \pi^+ \pi^+ \pi^- \pi^0$ | 4.0         | .275            | 1.10        |
| Total                         | 22.6        |                 | 8.59        |

TABLE III: The Cabibbo allowed (CA) branching ratio for various decays of the form  $D^0 \rightarrow K^- \pi^+ + n\pi$  are shown together with the acceptance as discussed above and the effective branching ratio. We will assume that the corresponding doubly-Cabibbo-suppressed (DCS) modes are equal to these multiplied by a factor of  $\sin^4 \theta_C$ . In the case of  $K^- \pi^0 \pi^+$  we have subtracted the portion which is produced via the  $K^{*-} \pi^+$  channel to avoid double counting with that mode.

events according to particle content or by analyzing the phase space distributions. In the early stages, however, such analysis may not give significant gains over treating these modes as inclusive ones.

In Table III we show the acceptance and effective branching ratios for various modes of this form. Note that we subtract  $\pi^+[K^{*-} \rightarrow K^- \pi^0]$  from the sample to avoid double counting. Again we will assume that the DCS modes are related by a factor of  $\sin^4 \theta_C$ . Because this is an inclusive state, we also need to specify the coherence factor  $R_F$  defined in the appendix. We will assume  $R_F = 0.51$  for our numerical illustration which is the value determined in the model discussed in [7]. The branching ratio to these modes via the CA channel are about 7 times that of  $\bar{D}^0 \rightarrow K^+ \pi^-$  with a similar ratio being true for the DCS analogs. Assuming the acceptance is roughly 1/2 of the two body decay, the number of events in this sample (106) is thus as shown in Table I.

In summary, we will investigate the determination of  $\gamma$  through considering various combinations of the following types of data shown in Table I:

1.  $D^0 \rightarrow K^+ \pi^-$ .
2.  $D^0 \rightarrow K^{*+} \pi^-$ .
3. GLW modes, i.e.  $D^0 \rightarrow CPES$ .
4. Inclusive decays of the form  $D^0 \rightarrow K^+ \pi^- + n\pi$ .
5. Singly Cabibbo Suppressed  $D$  decays such as  $D^0 \rightarrow K^{*\pm} K^\mp$ .
6. A determination of  $B^- \rightarrow K^- \bar{D}^0$  via a semi-leptonic tag of  $\bar{D}^0$ .
7. A determination of strong phases and the coherence factor,  $R_F$ , from a  $\psi(3770)$  charm factory

These will be combined with the following decays of the initial  $B$  meson:

1.  $B^- \rightarrow K^{(*)-} \mathbf{D}^{(*)0}$
2.  $B^- \rightarrow K^- \mathbf{D}^0 + X$
3.  $B^- \rightarrow [K^{*-} \rightarrow K^- \pi^0] \mathbf{D}^0 + X$

The accuracy in determining  $\gamma$  will, in general, depend on the value of  $\gamma$ , the strong phase of the  $B$  decay and the strong phase of the  $D$  decays. Clearly, these quantities are unknown and cannot be calculated. We are thus driven to consider sample calculations with arbitrarily chosen strong phases in order to project how the measurement will proceed.

For our sample calculations we will assume that  $\gamma = 60^\circ$  which is consistent with current data [24]. The strong phase differences for the various  $B$  and  $D$  decays we will use in our illustrative calculations are chosen completely arbitrarily and are given in Table IV. The table gives the strong phase difference between the  $B$  decay involving a  $D^0$  in the first column and the corresponding decay involving  $\bar{D}^0$  in the second column. Note that in the case of  $B^- \rightarrow K^{*-} \mathbf{D}^{*0}$  there are three different helicity amplitudes, helicity  $h = +1, 0$ , and  $-1$ , hence there are three different strong phases.

In order to carry forward our analysis we will need to make some assumptions concerning branching ratios of decays which have not been measured yet. In Table V we summarize the branching ratios for the decays which we use. The decays which are measured are taken from [18] and indicated by (\*) and the ones which we estimate are indicated by (†).

| Decay 1                                | Decay 2                                      | Phase Difference      |
|--|--|-----------------------|
| $B^- \rightarrow D^0 K^-$              | $B^- \rightarrow D^0 K^-$                    | $-50^\circ$           |
| $B^- \rightarrow D^{*0} K^-$           | $B^- \rightarrow D^{*0} K^-$                 | $-10^\circ$           |
| $B^- \rightarrow D^0 K^{*-}$           | $B^- \rightarrow \bar{D}^0 K^{*-}$           | $+30^\circ$           |
| $B^- \rightarrow D^{*0} K_{h=+1}^{*-}$ | $B^- \rightarrow \bar{D}^{*0} K_{h=+1}^{*-}$ | $+70^\circ$           |
| $B^- \rightarrow D^{*0} K_{h=0}^{*-}$  | $B^- \rightarrow \bar{D}^{*0} K_{h=+1}^{*-}$ | $+110^\circ$          |
| $B^- \rightarrow D^{*0} K_{h=-1}^{*-}$ | $B^- \rightarrow \bar{D}^{*0} K_{h=+1}^{*-}$ | $+150^\circ$          |
| $B^0 \rightarrow D^0 K^{*0}$           | $B^- \rightarrow D^0 K^{*0}$                 | $130^\circ$           |
| $B^0 \rightarrow D^{*0} K_{h=+1}^{*0}$ | $B^- \rightarrow \bar{D}^{*0} K_{h=+1}^{*0}$ | $+50^\circ$           |
| $B^0 \rightarrow D^{*0} K_{h=0}^{*0}$  | $B^- \rightarrow \bar{D}^{*0} K_{h=+1}^{*0}$ | $+10^\circ$           |
| $B^0 \rightarrow D^{*0} K_{h=-1}^{*0}$ | $B^- \rightarrow \bar{D}^{*0} K_{h=+1}^{*0}$ | $-30^\circ$           |
| $B^- \rightarrow D^0 K^- + X$          | $B^- \rightarrow \bar{D}^0 K^- + X$          | $45^\circ R = 0.7$    |
| $B^0 \rightarrow D^0 K^- + X$          | $B^0 \rightarrow \bar{D}^0 K^- + X$          | $135^\circ R = 0.7$   |
| $D^0 \rightarrow K^+ \pi^-$            | $D^0 \rightarrow K^+ \pi^-$                  | $+120^\circ$          |
| $D^0 \rightarrow K^+ \pi^- + n\pi$     | $D^0 \rightarrow K^+ \pi^- + n\pi$           | $+90^\circ (R = 0.5)$ |
| $D^0 \rightarrow K^{*+} \pi^-$         | $D^0 \rightarrow K^{*+} \pi^-$               | $+60^\circ$           |
| $D^0 \rightarrow K^{*+} K^-$           | $D^0 \rightarrow K^{*+} K^-$                 | $+30^\circ$           |

TABLE IV: The strong phase differences used in our sample calculations. The strong phase difference is between decay 1 involving  $D^0$  and decay 2 involving  $\bar{D}^0$ .

| Decay   | Branching Ratio       | Status |
|---|-----------------------|--------|
| $D^0 \rightarrow K^+ \pi^-$                             | 3.80%                 | *      |
| $D^0 \rightarrow K^+ \pi^-$                             | $1.48 \times 10^{-4}$ | *      |
| $D^0 \rightarrow K^{*+} \pi^-$                          | 6.0%                  | *      |
| $D^0 \rightarrow K^{*+} \pi^-$                          | $1.7 \times 10^{-4}$  | †      |
| $D^0 \rightarrow K^+ \pi^- + n\pi$                      | 25%                   | †      |
| $D^0 \rightarrow K^+ \pi^- + n\pi$                      | $7 \times 10^{-4}$    | †      |
| $D^0 \rightarrow CPES-$                                 | 5%                    | †      |
| $D^0 \rightarrow K^{*-} K^-$                            | 0.380%                | *      |
| $D^0 \rightarrow K^{*-} K^-$                            | 0.220%                | *      |
| $B^- \rightarrow K^- D^0$                               | $3.7 \times 10^{-4}$  | *      |
| $B^- \rightarrow K^{*-} D^0$                            | $6.1 \times 10^{-4}$  | *      |
| $B^- \rightarrow K^- D^{*0}$                            | $3.6 \times 10^{-4}$  | *      |
| $B^- \rightarrow K^{*-} D^{*0}$                         | $7.2 \times 10^{-4}$  | *      |
| $B^- \rightarrow K^- D^0$                               | $5.4 \times 10^{-6}$  | †      |
| $B^- \rightarrow K^{*-} D^0$                            | $9.0 \times 10^{-6}$  | †      |
| $B^- \rightarrow K^- D^{*0}$                            | $5.3 \times 10^{-6}$  | †      |
| $B^- \rightarrow K^{*-} D^{*0}$                         | $1.06 \times 10^{-5}$ | †      |
| $B^0 \rightarrow [K^{*0} \rightarrow K^- \pi^+] D^0$    | $4.6 \times 10^{-5}$  | †      |
| $B^0 \rightarrow [K^{*0} \rightarrow K^- \pi^+] D^{*0}$ | $5.5 \times 10^{-5}$  | †      |
| $B^0 \rightarrow [K^{*0} \rightarrow K^- \pi^+] D^0$    | $6.0 \times 10^{-6}$  | †      |
| $B^0 \rightarrow [K^{*0} \rightarrow K^- \pi^+] D^{*0}$ | $7.0 \times 10^{-6}$  | †      |

TABLE V: Branching ratios for various  $B$  and  $D$  decays. Those from [18] are indicated by \* while those which have been estimated have been indicated by †.

### III. CP ASYMMETRIES

For a given decay of the form  $B^- \rightarrow K^{(*)-} [D^{(*)0} \rightarrow F]$  where  $F$  is in general an exclusive or inclusive final state, let us denote

|                                 | $K^+\pi^-$ | $K^{*+}\pi^-$ | $K^+\pi^- + n\pi$ | $CPES-$ | $K^{*+}K^-$ | $K^{*-}K^+$ |
|---------------------------------|------------|---------------|-------------------|---------|-------------|-------------|
| $B^- \rightarrow K^- D^0$       | 29         | 53            | 165               | 1646    | 70          | 51          |
| $B^- \rightarrow K^{*-} D^0$    | 28         | 64            | 219               | 2636    | 74          | 44          |
| $B^- \rightarrow K^- D^{*0}$    | 22         | 47            | 147               | 1530    | 66          | 53          |
| $B^- \rightarrow K^{*-} D^{*0}$ | 40         | 53            | 244               | 3590    | 44          | 45          |

TABLE VI: The calculated branching ratio,  $d_{av} = (d + \bar{d})/2$  in units of  $10^{-8}$  for the combination of the various  $B^- \rightarrow K^{(*)-} D^{(*)0}$  decays in the left column with the  $D^0$  decays in the top row using the parameters from Table IV, where the strong phases were chosen arbitrarily. As indicated, the results are averaged over each decay chain and its charge conjugate.

|                                 | $K^+\pi^-$ | $K^{*+}\pi^-$ | $K^+\pi^- + n\pi$ | $CPES-$ | $K^{*+}K^-$ | $K^{*-}K^+$ |
|---------------------------------|------------|---------------|-------------------|---------|-------------|-------------|
| $B^- \rightarrow K^- D^0$       | 22         | 12            | 63                | 905     | 13          | 9           |
| $B^- \rightarrow K^{*-} D^0$    | 21         | 14            | 83                | 1450    | 13          | 8           |
| $B^- \rightarrow K^- D^{*0}$    | 17         | 11            | 56                | 842     | 12          | 10          |
| $B^- \rightarrow K^{*-} D^{*0}$ | 30         | 12            | 93                | 1974    | 8           | 8           |

TABLE VII: The branching ratio  $d_{av}$ , in units of  $10^{-8}$ , as in Table VI with the acceptance (not including  $R_{cut}$ ) folded in.

$$\begin{aligned}
d &= Br(B^- \rightarrow K^{(*)-} [D^{(*)0} \rightarrow F]) \\
\bar{d} &= Br(B^+ \rightarrow K^{(*)+} [D^{(*)0} \rightarrow \bar{F}])
\end{aligned}
\tag{3}$$

where in the case of  $\mathbf{D}^{*0}$  it cascades down to  $\mathbf{D}^0$  before a  $\mathbf{D}^0 \rightarrow F$  decay. In terms of the  $B$  and  $D$  branching ratios and the strong and weak phases, these quantities are given by

$$\begin{aligned}
d &= ac_F + b\bar{c}_F + 2R_F \sqrt{ac_F b\bar{c}_F} \cos(\zeta_B + \zeta_F + \gamma) \\
\bar{d} &= ac_F + b\bar{c}_F + 2R_F \sqrt{ac_F b\bar{c}_F} \cos(\zeta_B + \zeta_F - \gamma)
\end{aligned}
\tag{4}$$

where  $a = Br(B^- \rightarrow K^{(*)-} D^{(*)0})$ ,  $b = Br(B^- \rightarrow K^{(*)-} \bar{D}^{(*)0})$ ,  $\zeta_B$  is the strong phase difference of the  $B^-$  decay,  $\zeta_F$  is the strong phase difference for the  $D^0$  decay and  $R_F$  is the coherence factor as defined in [7]; in particular, for exclusive states  $R_F = 1$ . In the appendix, these expressions are generalized to the case where  $D^0 \bar{D}^0$  mixing is present.

For each decay, let us define

$$\begin{aligned}
d_{av} &= (d + \bar{d})/2 \\
A_{CP} &= (d - \bar{d})/(d + \bar{d})
\end{aligned}
\tag{5}$$

thus,  $A_{CP}$  is the CP violating asymmetry.

In Table VI we show the values of  $d_{av}$  which result from the parameters of our sample calculation in units of  $10^{-8}$ . In Table VIII we show the corresponding CP asymmetry  $A_{CP}$ . In an *ideal* detector, the number of  $B\bar{B}$  pairs required to observe the signal of CP violation (for definiteness, with a  $3\sigma$  statistical error) is:

|                                 | $K^+\pi^-$ | $K^{*+}\pi^-$ | $K^+\pi^- + n\pi$ | $CPES-$ | $K^{*+}K^-$ | $K^{*-}K^+$ |
|---------------------------------|------------|---------------|-------------------|---------|-------------|-------------|
| $B^- \rightarrow K^- D^0$       | -58.2%     | -8.1%         | -17.9%            | -17.1%  | -17.1%      | 14.3%       |
| $B^- \rightarrow K^{*-} D^0$    | -54.3%     | -63.3%        | -30.1%            | +11.6%  | -15.0%      | 13.4%       |
| $B^- \rightarrow K^- D^{*0}$    | -76.9%     | -39.4%        | -30.2%            | -4.1%   | -12.1%      | 8.1%        |
| $B^- \rightarrow K^{*-} D^{*0}$ | +58.4%     | -13.5%        | 10.7%             | +15.8%  | +14.6%      | -7.2%       |

TABLE VIII: The CP asymmetry  $A_{CP} = (d - \bar{d})/(d + \bar{d})$  corresponding to the results in Table VI is given.

|                                 | $K^+\pi^-$ | $K^{*+}\pi^-$ | $K^+\pi^- + n\pi$ | $CPES-$ | $K^{*+}K^-$ | $K^{*-}K^+$ |
|---------------------------------|------------|---------------|-------------------|---------|-------------|-------------|
| $B^- \rightarrow K^- D^0$       | 0.92       | 25.88         | 1.70              | 0.19    | 4.40        | 8.63        |
| $B^- \rightarrow K^{*-} D^0$    | 1.09       | 0.35          | 0.45              | 0.25    | 5.41        | 11.39       |
| $B^- \rightarrow K^- D^{*0}$    | 0.69       | 1.23          | 0.67              | 3.50    | 9.31        | 25.88       |
| $B^- \rightarrow K^{*-} D^{*0}$ | 0.66       | 9.32          | 3.22              | 0.10    | 9.60        | 38.58       |

TABLE IX: The number  $\hat{N} = 9/(d_{av}A_{CP}^2)$  of  $B\bar{B}$  pairs needed to see a  $3 - \sigma$  signal of CP-violation in units of  $10^8$ ; detection efficiencies, acceptances etc are *not* included in these numbers but are included in Table X.

|                                 | $K^+\pi^-$ | $K^{*+}\pi^-$ | $K^+\pi^- + n\pi$ | $CPES-$ | $K^{*+}K^-$ | $K^{*-}K^+$ |
|---------------------------------|------------|---------------|-------------------|---------|-------------|-------------|
| $B^- \rightarrow K^- D^0$       | 6.05       | 508           | 22.4              | 1.73    | 122         | 240         |
| $B^- \rightarrow K^{*-} D^0$    | 7.17       | 7.95          | 5.92              | 2.27    | 150         | 306         |
| $B^- \rightarrow K^- D^{*0}$    | 4.53       | 28.0          | 8.82              | 31.8    | 259         | 722         |
| $B^- \rightarrow K^{*-} D^{*0}$ | 4.34       | 211           | 42.4              | 0.9     | 267         | 1083        |

TABLE X: The number  $N = 9/(d_{av}A_{CP}^2)$  of  $B\bar{B}$  pairs needed to see a  $3 - \sigma$  signal of CP-violation in units of  $10^8$  taking into account the detection efficiencies, acceptances discussed in the text and assuming  $R_{cut} = 0.2$ ; see Eq. 1.

$$\hat{N} = \frac{9}{d_{av}A_{CP}^2} \quad (6)$$

Tables (IX,X) indicate the number of  $B\bar{B}$  pairs which would be required to observe a  $3 - \sigma$  signal of CP violation in these modes; Table X includes efficiencies and acceptance factors as given in Eq. 1. From these tables it can be seen that with a  $(1 - 10) \times 10^8$   $B$ 's CP violation can be seen in several individual channels. In Table XI we show the values of  $d_{av}$  where we average over strong phases but keep  $\gamma = 60^\circ$ ; likewise in Table XII we show the r.m.s averaged values of  $|A_{CP}|$ . Comparing these to the specific results in Table VIII, obtained by assuming arbitrarily assigned values for strong phases, we see that the two approaches tend to give similar results. In Table XIII we show the r.m.s asymmetries where we have also averaged over  $\gamma$  where  $\gamma$  ranges from 0 to  $2\pi$ .

#### IV. EXTRACTING $\gamma$

We will now consider various strategies to determine  $\gamma$  assuming we experimentally observe the results given in Tables (VI,VIII) with the number of reconstructed events as discussed above.

First, let us consider in isolation the case of  $B^- \rightarrow K^- [D^0 \rightarrow K^+\pi^-]$ . This rate, together with its charge conjugate gives us two distinct observables which are determined in terms of four unknown parameters:  $\zeta_{KD}$ ,  $\zeta_{K^+\pi^-}$ ,  $b(KD)$  and  $\gamma$ . The two strong phases enter as the sum  $\zeta_{tot} = \zeta_{KD} + \zeta_{K^+\pi^-}$  so in effect there are only three parameters  $\{\zeta_{tot}, b(KD), \gamma\}$ . Still we cannot expect to reconstruct  $\gamma$  but, as discussed in [6], this data gives a bound on  $\sin^2 \gamma$ .

To illustrate this, in Fig. (2) the thin solid line shows the minimum value of  $\chi^2$  as a function of  $\gamma$ . For each value of  $\gamma$  we minimize with respect to the other parameters  $\{\zeta_{tot}, b(KD)\}$ . In the region of the graph where  $\gamma > 45.6^\circ$ ,  $\chi^2$  vanishes indicating that this is the lower bound within the first quadrant. Note that this and all similar graphs we will discuss are periodic with respect to  $\gamma \rightarrow \pi \pm \gamma$  so, for instance, in the second quadrant the bound is  $\gamma < 180^\circ - 45.6^\circ$  etc..

|                                 | $K^+\pi^-$ | $K^{*+}\pi^-$ | $K^+\pi^- + n\pi$ | $CPES-$ |
|---------------------------------|------------|---------------|-------------------|---------|
| $B^- \rightarrow K^- D^0$       | 26         | 38            | 161               | 1877    |
| $B^- \rightarrow K^{*-} D^0$    | 43         | 64            | 268               | 3095    |
| $B^- \rightarrow K^- D^{*0}$    | 25         | 38            | 158               | 1827    |
| $B^- \rightarrow K^{*-} D^{*0}$ | 51         | 76            | 315               | 3653    |

TABLE XI: The value of  $d_{av}$  is given using  $\gamma = 60^\circ$  and the branching ratios in Table V but with all of the strong phases taken at random.

|                                 | $K^+\pi^-$ | $K^{*+}\pi^-$ | $K^+\pi^- + n\pi$ | $CPES-$ |
|---------------------------------|------------|---------------|-------------------|---------|
| $B^- \rightarrow K^- D^0$       | 53.4%      | 47.7%         | 47.5%             | 14.6%   |
| $B^- \rightarrow K^{*-} D^0$    | 53.4%      | 47.7%         | 47.5%             | 14.6%   |
| $B^- \rightarrow K^- D^{*0}$    | 53.4%      | 47.7%         | 47.5%             | 14.6%   |
| $B^- \rightarrow K^{*-} D^{*0}$ | 36.8%      | 33.0%         | 23.0%             | 10.4%   |

TABLE XII: The r.m.s. average of  $|A_{CP}|$  corresponding to the results in Table XI.

|                                 | $K^+\pi^-$ | $K^{*+}\pi^-$ | $K^+\pi^- + n\pi$ | $CPES-$ |
|---------------------------------|------------|---------------|-------------------|---------|
| $B^- \rightarrow K^- D^0$       | 44.3%      | 39.3%         | 39.1%             | 12.0%   |
| $B^- \rightarrow K^{*-} D^0$    | 44.3%      | 39.3%         | 39.1%             | 12.0%   |
| $B^- \rightarrow K^- D^{*0}$    | 44.3%      | 39.3%         | 39.1%             | 12.0%   |
| $B^- \rightarrow K^{*-} D^{*0}$ | 30.3%      | 27.1%         | 18.8%             | 8.5%    |

TABLE XIII: The results as in Table XII averaged over all values of  $\gamma$  (from 0 to  $2\pi$ ).

Clearly, in this case, the data is too meager to provide a useful bound. The  $3\sigma$  bound (i.e. where  $\chi^2 \approx 9$ ) is only slightly above 0.

We can also consider the bound on  $\gamma$  obtained from the decay  $D^0 \rightarrow CPES-$  in isolation. There are more events of this type but the power this data to bound  $\gamma$  is not much greater since  $A_{CP}$  is smaller (in general we expect the analyzing power of a particular mode to be  $\sim A_{CP}^2$ ). The minimum  $\chi^2$  in this case is shown with the dotted curve. Notice that taken in isolation it seems to be worse than even the single  $D^0 \rightarrow K^+\pi^-$  (CPNES) mode.

Of course both of these two data sets depend on the common parameter  $b$  and if we have both sets of data together we obtain the results shown with thick solid curve which is an improvement on each of the data sets taken in isolation; in fact this thick solid curve gives a  $3\sigma$  bound of  $\gamma > 16^\circ$ . As discussed in [5] since there the number of equations and observables is the same, there are ambiguous solutions which leads to the  $\chi^2$  value being small over an extended range.

To improve the situation, we can also use data from all four decays of the form  $B^- \rightarrow K^{(*)-} D^{(*)0}$ . Note that

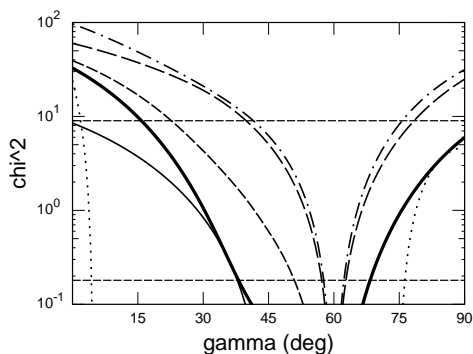


FIG. 2: The minimum value of  $\chi^2$  is shown as a function of  $\gamma$  for various combinations of data in the sample calculation. The thin solid line shows the result using just  $B^- \rightarrow K^- [D^0 \rightarrow K^+\pi^-]$  data. The dotted line shows the result using just the  $B^- \rightarrow K^- [D^0 \rightarrow CPES-]$  data. The thick solid curve shows the result taking both  $B^- \rightarrow K^- [D^0 \rightarrow K^+\pi^-]$  and  $B^- \rightarrow K^- [D^0 \rightarrow CPES-]$  data together. The dashed line shows the result using  $B^- \rightarrow K^{(*)-} [D^{(*)0} \rightarrow K^+\pi^-]$ . In the dash dotted curve, all four of the initial  $B^-$  decays where the  $D$  decays to the same two final states are considered. Thus the dashed dotted curve results from taking together data of the form  $B^- \rightarrow K^{(*)-} [D^{(*)0} \rightarrow K^+\pi^-]$  and  $B^- \rightarrow K^{(*)-} [D^{(*)0} \rightarrow CPES-]$ . The long dashed curve only includes data from two parent  $B^-$  decays, i.e.  $B^- \rightarrow K^- D^0$  as well as  $B^- \rightarrow K^- [D^{*0} \rightarrow D^0 + \pi^0(\gamma)]$  with either of the two  $D^0$  decaying to  $K^+\pi^-$  as well as  $CPES-$ . The upper horizontal dashed line indicates the 3-sigma level determination of  $\gamma$  with the luminosity required to give the results in Table I which corresponds to current B-factories while the lower horizontal dashed line corresponds to a luminosity 50 times greater which may be achieved at future high luminosity B factories.

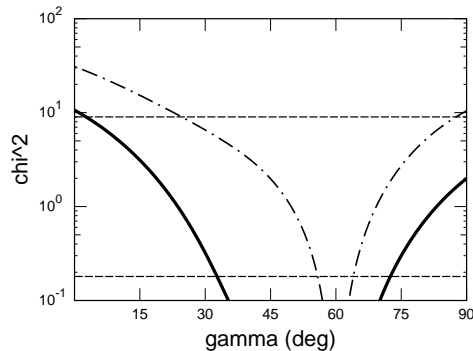


FIG. 3: The minimum value of  $\chi^2$  using the four SCS modes in Eqn. (2) is shown with the solid line. The dashed dotted line shows the results with  $D^0 \rightarrow K^{*+}K^-$  and  $D^0 \rightarrow K^{*-}K^+$  together with the four parent  $B^- \rightarrow \mathbf{D}^{(*)0}K^{(*)-}$  decays.

each of these modes will have a different unknown value of  $b$  and  $\zeta$ . In addition, the decay mode  $K^*-D^0$  has three polarization amplitudes which we will take into account by introducing a coherence factor  $R_F$  into the fit since we are assuming that we are only observing the sum and we do not consider the additional information that could be determined from the angular distributions of the decays of the vectors as discussed in [8]. If we consider the single decay  $D^0 \rightarrow K^+\pi^-$  we obtain the results shown by the dashed line which in this case gives a  $3-\sigma$  bound on  $\gamma$  of  $\gamma > 23^\circ$ . The dot dash curve shows the result where we have both the  $D^0 \rightarrow K^+\pi^-$  and  $D^0 \rightarrow CPES-$  data. In this case we obtain a  $3-\sigma$  determination of  $\gamma$  (within the first quadrant) to be  $60_{-19.5}^{+15.5}$ . Using the additional data improved the situation both by providing more statistics and because the different data sets have different spurious solutions leaving only the correct solution in common.

For this dash-dot curve it is instructive to examine the number of observables versus the number of unknown free parameters. First of all, for  $\mathbf{D}^0 \rightarrow K^+\pi^-$  there is the strong phase. For each of the four parent  $B^-$  decays there is a strong phase. In the case of  $B^- \rightarrow K^*-\mathbf{D}^{*0}$  there is, in addition, a parameter  $R$ . Again, for each of the four parent decays there is the unknown branching ratio  $b = Br(B^- \rightarrow K^{(*)-}\mathbf{D}^{*0})$  and finally the angle  $\gamma$  giving a total of 11 parameters. On the other hand, for each combination of  $B$  and  $D$  decays there are two observables,  $d$  and  $\bar{d}$  giving a total of 16 so there is an overdetermination by 5 degrees of freedom.

As another example, consider the case where only two the four combinations of  $B^- \rightarrow K^{(*)-}\mathbf{D}^{(*)0}$  are observed with  $D$  decay to  $K^+\pi^-$  and  $CPES-$ , then the system is still overdetermined. In Fig. 2 the long dashed line takes into account only the two  $B^- \rightarrow K^-\mathbf{D}^0$  and  $B^- \rightarrow K^-\mathbf{D}^{*0}$  and so has 6 unknown parameters determined by 8 observables. Clearly having some overdetermination is helpful in obtaining a good determination of  $\gamma$ .

It is important to contrast thick solid curve with the long dashed one, in Fig. 2. Recall both of them have  $\mathbf{D}^0 \rightarrow K^+\pi^-$ ,  $CPES-$ . However, in case of the thick solid curve the  $\mathbf{D}^0$  originate only from  $B^- \rightarrow K^-\mathbf{D}^0$  whereas the long dashed curve is also getting the  $\mathbf{D}^0$  coming from  $\mathbf{D}^{*0} \rightarrow \mathbf{D}^0 + \pi^0(\gamma)$ . As a result whereas in the thick solid case there are 4 observables and 4 unknowns for the long-dashed case its 8 observables for 6 unknowns. That ends up making a significant difference as is evident from the figure; a lot more than one may naively expect just by doubling the number of  $\mathbf{D}^0$  or a factor of two in luminosity. Infact the lower horizontal line in Fig. 2 indicates (which corresponds to  $3-\sigma$  determination at high luminosity) that the reduction in error on  $\gamma$  is roughly a factor of 5 (between the thick solid and the long-dashed curves), i.e. a saving in effective luminosity of a factor of about 25.

It is also instructive to compare dash-dot curve, which clearly has substantially more data, with the long-dash one. Notice that quality of determination of  $\gamma$  by the two data sets is about the same. This suggests that once the number of observables is sufficiently large to overdetermine the parameters, further gains by including additional information only leads to modest gains.

We can also determine  $\gamma$  by using the four SCS modes in Eqn. (2). In Fig. 3 we show  $\chi^2$  using these modes. If we again consider the four parent decays  $B^- \rightarrow D^{(*)0}K^{(*)-}$  then we obtain the results shown with the dashed dotted line which roughly gives  $\gamma > 30^\circ$  as a  $3\sigma$  bound.

Let us now consider additional sources of information which could constrain these results. In the next section we will discuss the impact of flavor tagging the  $\mathbf{D}^0$  by means of semileptonic decays. This is challenging but may be possible at  $B$  factories. Apart from  $B$  factory data, another source of additional information discussed in [7], is to use the charm factory to determine the strong phase differences  $\zeta_F$  as well as  $R_F$  for inclusive modes. In Fig 4 the thick solid line shows the results using  $B^- \rightarrow K^-\mathbf{D}^0$  followed by  $D^0$  decay to  $K^+\pi^-$  and  $CPES-$  as Fig 2. The thin solid line shows the result if we suppose that we have the phase  $\zeta_{K^+\pi^-}$  determined by a  $\psi(3770)$  charm factory.

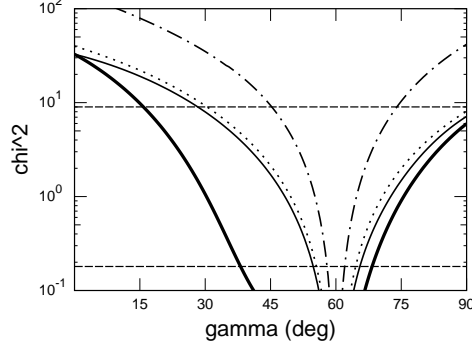


FIG. 4: The thick solid curve shows  $\chi^2$  as a function of  $\gamma$  taking both  $B^- \rightarrow K^-[\mathbf{D}^0 \rightarrow K^+\pi^-]$  and  $B^- \rightarrow K^-[\mathbf{D}^0 \rightarrow CPES-]$  data together as in Fig. 2. The thin solid curve shows the result if  $\zeta_{K^+\pi^-}$  is determined separately at a  $\psi(3770)$  charm factory. The dotted curve includes  $B^- \rightarrow K^-[\mathbf{D}^0 \rightarrow K^+\pi^-]$   $B^- \rightarrow K^-[\mathbf{D}^0 \rightarrow K^{*+}\pi^-]$   $B^- \rightarrow K^-[\mathbf{D}^0 \rightarrow K^+\pi^- + n\pi]$   $B^- \rightarrow K^-[\mathbf{D}^0 \rightarrow CPES-]$  as well as the phase determination from a  $\psi(3770)$  charm factory. The dashed dotted curves considers all these decay modes together with the four parent decays  $B^- \rightarrow K^{*-}D^{*0}$  as well as phase determination from a  $\psi(3770)$  charm factory.

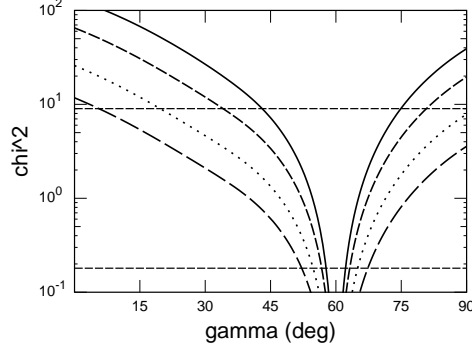


FIG. 5: The results for  $B^- \rightarrow K^{(*)-}D^{(*)0}$  followed by  $\mathbf{D}^0 \rightarrow K^+\pi^-; CPES-; K^+\pi^- + n\pi, K^{*+}\pi^-$  where finite CP conserving backgrounds are included. The solid curve is for no background; the dashed curve is for signal/background=1, the dotted curve is for signal/background= $\frac{1}{4}$  and the long dashed curve is for signal/background= $\frac{1}{10}$

Clearly this improves the situation by removing the ambiguities. Of course the situation can be improved still further by including several different  $D$  decay modes. In the dotted line, we show the result where we use  $\psi(3770)$  data with the modes  $K^+\pi^-$ ,  $K^{*+}\pi^-$  and  $CPES-$  and, in addition, the inclusive decay  $D^0 \rightarrow K^+\pi^- + n\pi$ . Note that as well as determining the strong phase difference for all the  $D^0$  decays, the  $\psi(3770)$  data also determines the value of  $R_F$  for  $F = K^+\pi^- + n\pi$ . As before, we can also improve the situation by combining the data from all  $B^- \rightarrow K^{(*)-}D^{(*)0}$  combinations as is shown by the dot dashed line. In this case, the determination of  $\gamma$  ( $3\sigma$ ) is  $60 \pm 10^\circ$ .

In the above, we have assumed that there is no background. In general, of course, there should be a CP-even background which will tend to increase the error in  $\gamma$ . In Fig. (5) we show the  $\chi^2$  as a function of  $\gamma$  for all four modes including all the combinations of  $B^- \rightarrow K^{(*)-}D^{(*)0}$  with the solid line. The dashed line shows the results with a signal/background ratio of 1; the dotted line shows the result for signal/background is  $\frac{1}{4}$  while the long dashed curve shows the result for signal/background is  $\frac{1}{10}$ .

The  $3-\sigma$  errors in  $\gamma$  in these cases is  $60_{-16.0}^{+15.1}^\circ$  for no background and  $60_{-26.1}^{+20.8}^\circ$  for signal/background=1.

Recall that the color suppressed branching ratios for  $B^- \rightarrow K^-\bar{D}^0$  and  $B^- \rightarrow K^{*-}\bar{D}^0$  are likely to be very difficult to measure experimentally (see however section V). The above analysis[5, 6] is therefore designed to yield both these suppressed Br's as well as  $\gamma$  with the input of each data set. Fig. 6 serves to illustrate how well this works out using data for all the combinations of  $B^- \rightarrow K^{(*)-}D^{(*)0}$  followed by  $\mathbf{D}^0 \rightarrow K^+\pi^-; CPES-; K^+\pi^- + n\pi, K^{*+}\pi^-$ . The dependence on  $Br(B^- \rightarrow K^-\bar{D}^0)$  is indicated by the solid line while the dependence on  $Br(B^- \rightarrow K^{*-}\bar{D}^0)$

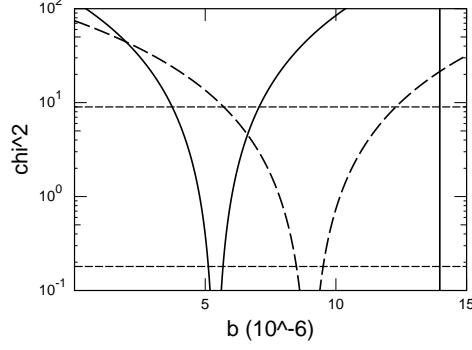


FIG. 6: The minimum value of  $\chi^2$  is shown as a function of  $Br(B^- \rightarrow K^- \bar{D}^0)$  and  $Br(B^- \rightarrow K^{*-} \bar{D}^0)$  using data for all the combinations of  $B^- \rightarrow K^{(*)-} \mathbf{D}^{(*)0}$  followed by  $\mathbf{D}^0 \rightarrow K^+ \pi^-$ ;  $CPES-$ ;  $K^+ \pi^- + n\pi$ ,  $K^{*+} \pi^-$ . The dependence on  $Br(B^- \rightarrow K^- \bar{D}^0)$  is indicated by the solid line while the dependence on  $Br(B^- \rightarrow K^{*-} \bar{D}^0)$  is shown by the dashed curve.

is shown by the dashed curve. The 3-sigma determination of  $Br(B^- \rightarrow K^- \bar{D}^0)$  is thus  $\approx \pm 1.8 \times 10^{-6}$  and for  $Br(B^- \rightarrow K^{*-} \bar{D}^0)$  it is  $\approx \pm 2.25 \times 10^{-6}$ .

## V. FLAVOR TAGGING $D^0$ MESONS VIA SEMILEPTONIC DECAYS

Clearly a very useful constraint on the system of equations Eqn. (4) would be a direct determination of the branching ratio,  $b = Br(B^- \rightarrow K^- \bar{D}^0)$ . This can only be done if one observes the  $\bar{D}^0$  decay to a flavor specific semi-leptonic decay [5]. Unfortunately this is subject to a large background from semi-leptonic decays of the parent  $B^-$  since both semi-leptonic decays result in negatively charged leptons.

The kinematics of the two kinds of processes are, however, quite different so it may eventually be possible to determine  $b$ . As a case in point let us examine the kinematics involved if one considers  $B^- \rightarrow K^- \bar{D}^0$  followed by  $\bar{D}^0 \rightarrow \ell^- \bar{\nu}_\ell K^+$ .

First of all,  $\sum_{\ell=e,\mu} Br(\bar{D}^0 \rightarrow \ell^- \bar{\nu}_\ell K^+) = 6.9\%$ , hence the combined branching ratio using the estimate in Table V is:

$$\sum_{\ell=e,\mu} Br(B^- \rightarrow K^- [\bar{D}^0 \rightarrow \ell^- \bar{\nu}_\ell K^+]) = 3.7 \times 10^{-7} \quad (7)$$

The final state for this signal is thus  $\bar{\nu}_\ell K^+ K^-$  and it will be subject to the following backgrounds (including  $l = e$  and  $\mu$ ) :

- (a) The semi-leptonic decay  $B^- \rightarrow \bar{\nu}_\ell [D^0 \rightarrow K^+ K^-]$ . This has a combined branching ratio of  $1.7 \times 10^{-4}$ .
- (b) The semi-leptonic decay  $B^- \rightarrow \bar{\nu}_\ell [D^0 \rightarrow \pi^+ K^-]$  where the  $\pi^+$  is misidentified as a  $K^+$ . The combined branching ratio is  $1.6 \times 10^{-3}$ . Of course this must be multiplied by the rate of mis-identification for a given state.
- (c)  $B^- \rightarrow \bar{\nu}_\ell + [X_c \rightarrow K^+ K^- + X]$ , with a branching ratio  $\approx (10^{-2} - 10^{-3})$ .
- (d)  $B^- \rightarrow \bar{\nu}_\ell K^+ K^-$ ; the branching ratio is crudely estimated to be around  $3 \times 10^{-5}$ .
- (e) Backgrounds form continuum events

Against these backgrounds one can apply the following kinematic cuts.

- (1) For the signal the energy of the  $K^-$  in the rest frame of the  $B^-$  is fixed to be  $E_{K^-} = (m_B^2 + m_K^2 - m_D^2)/(2m_B)$ .
- (2) The missing neutrino leads to the constraint  $|p_B - p_{K^-} - p_\ell - p_{K^+}| = 0$ .

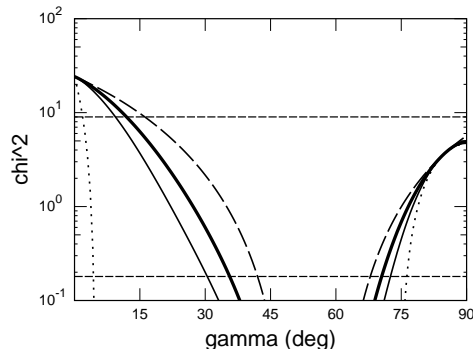


FIG. 7:  $\chi^2$  as a function of  $\gamma$  for  $B^- \rightarrow K^- [D^0 \rightarrow CPES-]$ . The dotted curve is the same as in Fig. 2, the long dashed curve assumes that  $b$  has a 10% 1- $\sigma$  error, the thick line assumes a 100% error and the thin solid line assumes a 200% error.

- (3) For backgrounds of the type (a), the invariant mass of the  $K^+K^-$  system will be  $m_D$ ; indeed, to eliminate the related backgrounds from  $D^0 \rightarrow K^+K^- + X$  one may use the cut  $|p_{K^+} + p_{K^-}| > m_D$ .
- (4) Signal events will have three distinct vertices while continuum background will have only 1.

Background (a) and (b) are  $\sim 10^3 \times$  signal. Cut (3) would remove these entirely except for momentum resolution but the additional cuts (1) and (2) which are satisfied by the signal may be sufficient to control this large background. Backgrounds (d) is probably  $O(10^2)$  times the signal; (c) is probably even a lot bigger. (d) in particular would pass cuts (2) and (3) and would have to be reduced by cuts (1) and (4). Likewise background (c) would have to be reduced by the monoenergetic kaon cut (1). Background (e) could, in principle, also be large and it is not clear whether cuts (1) and (4) together with the standard cuts against the continuum can be sufficient to eliminate it.

In spite of the difficulty in determining  $b$ , in the case where the  $D^0$  decays to a CP eigenstate, a relatively weak bound, on  $b$ , can be helpful in a determination of  $\gamma$ .

In Fig. 7 we show the  $\chi^2$  curve obtained just from the GLW modes,  $B^- \rightarrow K^- [D^0 \rightarrow CPES-]$ , as in Fig. (2) with the dotted line. The dashed line, the thick solid line and the thin solid line correspond to the result obtained assuming a 10%, 100% and 200% 1- $\sigma$  Gaussian error in the determination of  $b$  respectively. These lead to 3- $\sigma$  lower bounds on  $\gamma$  of 25.2°, 16.8° and 12.6° with the prospect of improvement at higher statistics. The reason for this is that the CP violation in this case is relatively small  $\sim 15\%$  so that the solutions with small  $\gamma$  correspond to a situation where  $b$  is large but  $\zeta_B \sim 180^\circ$  so there is near cancellation between the two channels. This is quite different from the actual situation where  $b \ll a$  so a modest bound on  $b$  improves the situation greatly.

If an experimental value for  $b$  is not available, a theoretical estimate can serve at the expense of the result becoming model dependent. From the above, such an estimate need not be very precise to be of some utility. On the other hand, the decay  $B^- \rightarrow K^- \bar{D}^0$  is color suppressed making reliable theoretical predictions more difficult.

In Fig. 8 we show the analogous calculation where we have combined the data from all the combinations of  $B^- \rightarrow K^{(*)-} [D^{(*)0} \rightarrow CPES-]$  with a determination of  $b$  to 10% (thick solid line), 200% (dotted line) and unconstrained (dashed line). These give the corresponding 3-sigma lower bound on  $\gamma$  of 40.2°, 16.2° and 3° respectively and upper bounds of 76.8°, 78.0° and 78.6°, respectively.

## VI. IMPACT OF $D\bar{D}$ MIXING

As has been discussed previously in the literature [6, 21], the effects of  $D\bar{D}$  mixing could be significant on some of the combined branching ratios. This is particularly true for final states such as  $K^+\pi^-$  because the favored decay  $B^- \rightarrow K^- D^0$  could be followed by the favored  $\bar{D}^0 \rightarrow K^+\pi^-$  if the  $D^0$  were to oscillate to a  $\bar{D}^0$ . If the probability of oscillation is  $O(1\%)$  then this channel might be comparable to the direct DCS rate for  $B^- \rightarrow K^- [D^0 \rightarrow K^+\pi^-]$  which is assumed to be the only channel in the absence of oscillation.

As discussed in the appendix, mixing is controlled by 4 parameters,  $x$ ,  $y$ ,  $A$  and  $\phi$ . If CP is conserved in  $D$  decays, which is an excellent approximation in the SM, then  $A = \phi = 0$ . The standard model predicts that the parameter controlling the mass difference,  $x \sim O(10^{-4})$ . The Standard Model prediction for the parameter relevant for the life time difference,  $y$ , is less certain since it could be enhanced by final state hadronic interactions. It has been suggested [25] that  $y$  could be as large as  $10^{-2}$ .

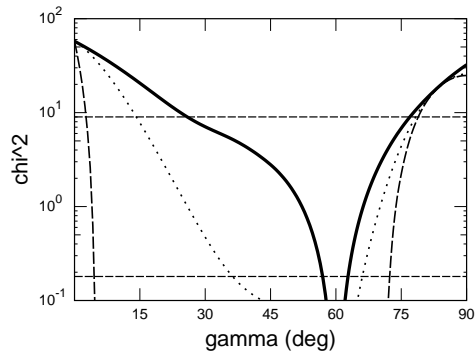


FIG. 8: The curves are as in Fig. 7 except all four  $B^-$  decays of the form  $B^- \rightarrow K^{(*)-} D^{*(0)}$  are considered.

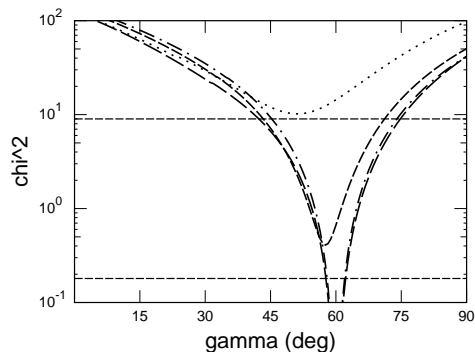


FIG. 9: The solid line shows the fit to the data from  $K^+\pi^-$ ,  $K^+\pi^- + n\pi$ ,  $CPES-$  and  $K^{*+}\pi^-$  with no  $D$  mixing. the dashed line shows the fit, assuming  $y = 0$  to the data in the case  $y = 0.01$  the dotted line shows the fit, assuming  $y = 0$  to the data in the case  $y = 0.1$  while the dash dotted line shows fit where a non-zero value of  $y$  is taken into account where the data is generated with  $y = 0.1$ .

In Fig. 9 the solid line is a fit to the data for  $K^+\pi^-$ ,  $K^+\pi^- + n\pi$ ,  $CPES-$  and  $K^{*+}\pi^-$  final states as discussed before. The dotted line shows the result if  $y = 0.01$  but the result is fit assuming there is no mixing. The minimum value of  $\chi^2$  has been shifted down to  $58^\circ$ . The dashed line shows the same calculation for  $y = 0.05$  and the minimum value of  $\chi^2$  is shifted down to  $51^\circ$ . The dashed dotted line shows the  $\chi^2$  for  $y = 0.05$  where the fit is done taking into account a non-zero value of  $y$ . In this case the fit value of  $\gamma$  is  $60^{+15.5}_{-16}^\circ$ .

Of course data from a  $\psi(3770)$  charm factory should be able to improve significantly on the constraints on the  $D^0\bar{D}^0$  mixing parameters and thereby it could immensely aid in the accurate determination of  $\gamma$  from the  $B \rightarrow KD^0$  method.

## VII. SELF TAGGING NEUTRAL $B$ DECAYS

It is also useful to add information obtainable from the decay of neutral  $B$ 's. Since  $B^0$  undergoes oscillation there are two strategies which can be considered:

- The  $B^0$  decays which are flavor non-specific such as  $B^0 \rightarrow K_S D^0$  or  $B^0 \rightarrow K^{*0} D^0$  where  $K^{*0} \rightarrow K_S \pi^0$ . In this case the oscillation of the  $B^0$  plays a role.
- Self-tagging [9, 10] decays which are flavor specific such as  $B^0 \rightarrow \bar{K}^{*0} D^0$  where  $K^{*0} \rightarrow K^- \pi^+$ . In this case the oscillation of the  $B^0$  does not play a role.

In the flavor non-specific case, the oscillation phase  $\beta$  in the Standard Model enters in such a way that the main dependence is on  $\delta \equiv 2\beta + \gamma \equiv \beta - \alpha + \pi$ . This has been discussed in [12, 13, 14, 15].

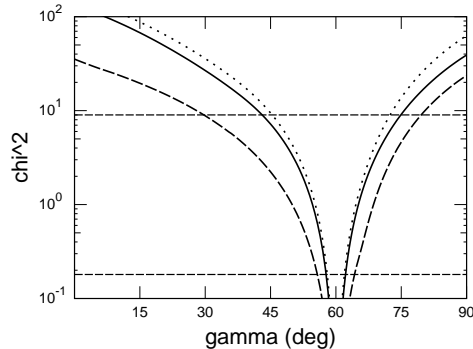


FIG. 10: The solid curve is generated using charged  $B^-$  data and is the same as the solid curve in Fig. 5 The dashed curve uses only neutral data with the two parent decays  $\bar{B}^0 \rightarrow [\bar{K}^{*0} \rightarrow K^- \pi^0] \mathbf{D}^{(*)0}$  and subsequent  $\mathbf{D}$  decay to  $K^+ \pi^-$ ,  $K^{*+} \pi^-$ ,  $K^+ \pi^- + n\pi$ ,  $CPES-$ . The dotted curve combines the data set used in the solid curve (charged  $B$ ) with the data set used in the dashed curve (neutral  $B$ ).

Here we will discuss the former case where the oscillation plays no role and so only direct CP violation via flavor specific decays is used in a determination of  $\gamma$ ; for instance, via the decay  $\bar{B}^0 \rightarrow [K^{*0} \rightarrow K^- \pi^+] \mathbf{D}^0$ . The main difference with the charged ( $B^\pm$ ) decay is that the  $b \rightarrow c$  channel is color suppressed and thus will be about 9 times smaller than the charged case. Thus we will estimate the branching ratios as shown in Table V. The  $b \rightarrow u$  channel proceeds via the same diagram in the charged and neutral cases hence the branching ratios in these cases should be about the same as shown in Table V.

Because of the suppression of the  $b \rightarrow c$  channel, if  $D^0$  decays to a DCS mode the amplitudes no longer are matched and so the CP violation will be somewhat smaller than in the charged case. Conversely the CP violation in modes with  $D$  decays to  $CPES$  will now be larger.

In Fig. 10 we illustrate the use of such modes. The solid line, for reference is the same as in Fig. 5, including data from all combinations of  $B^- \rightarrow K^{(*)-} \mathbf{D}^{(*)0}$  with subsequent  $\mathbf{D}$  decay to  $K^+ \pi^-$ ,  $K^{*+} \pi^-$ ,  $K^+ \pi^- + n\pi$ ,  $CPES-$ . The dashed curve considers the neutral  $B$  decays  $\bar{B}^0 \rightarrow [\bar{K}^{*0} \rightarrow K^- \pi^0]$  with subsequent  $\mathbf{D}$  decay to the same four final states. Because of the extra color suppression, it is not surprising that it falls below the solid line. Of course we can combine the two data sets since the strong phases of the  $\mathbf{D}$  decays should be common to each in which case one obtains the dotted curve improving the situation slightly over the solid curve.

### VIII. MULTIBODY $B$ DECAYS

Two body decay modes of the  $B$  to  $\mathbf{D}^0$  suffer from the problem that at least one of the channels is color suppressed. A method to circumvent this has been suggested by Aleksan, Petersen and Soffer (APS) [16] that decays of the form  $B^- \rightarrow K^- \pi^0 D^0$  may be used to extract  $\gamma$ . On the quark level the processes are the same as the two body  $B$  decays considered above but in this manifestation there are two important differences:

1. Both the  $b \rightarrow c$  and  $b \rightarrow u$  channels are color allowed.
2. The amplitude is a function of the 3-body phase space.

The fact that the  $b \rightarrow u$  channel is color allowed is important since it can improve the statistics, particularly if  $D$  decays to  $CPES$ . To take full advantage of this, however, we must overcome the fact that this is an inclusive state spread over phase space (i.e. the Dalitz Plot).

The APS method [16] is to extract from the data a number of different amplitudes and their relative phases by fitting to the Dalitz plot using a model with resonance and continuum terms and comparing the  $D^0$  decay to  $CPES$  and flavor specific modes.

Here we will consider a complimentary approach where we integrate over the Dalitz plot using the formalism of Eqn. (13) in the Appendix where there is an additional coherence parameter associated with the  $B$  decay. In this approach, though, several different three or more body decays may be taken together which will tend to increase the statistics.

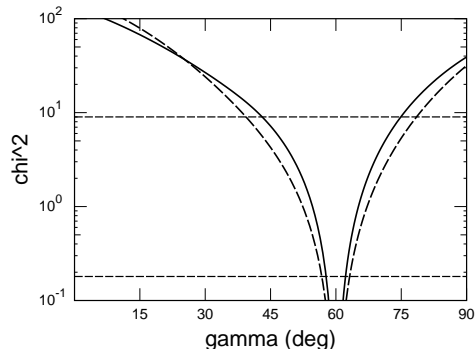


FIG. 11: The solid curve is the same as in Fig. 5 while the dashed one is the  $\chi^2$  for  $\gamma$  determined by the three body  $B^-$  decay modes  $\mathbf{D}^0 K^- \pi^0$ ,  $\mathbf{D}^{*0} K^- \pi^0$  and  $\mathbf{D}^0 K^{*-} \pi^0$  using the assumptions discussed in the text.

First, let us compare the number of degrees of freedom versus the number of observables in such a case. Suppose that we consider  $N$  inclusive decays of the form  $B \rightarrow \mathbf{D}^0 K + X_i$  ( $i = 1 \dots N$ ) where the  $\mathbf{D}^0$  subsequently decays into  $CPES-$ ,  $M_E$  exclusive modes and  $M_I$  inclusive modes. For each  $B$  decay there are 3 parameters,  $b$ ,  $\zeta$  and  $R_F$ . For each inclusive  $D$  mode there is one phase while for each inclusive  $D$  mode there is a phase and a coherence factor. In addition, of course,  $\gamma$  is also unknown giving  $3N + M_E + 2M_I + 1$  parameters. On the other hand, for each combination of  $B$  decay modes with each  $\mathbf{D}$  decay mode there are two observables,  $d$  and  $\bar{d}$  giving a total of  $2N(M_E + M_I + 1)$  observables. Thus,  $\gamma$  may be determined if

$$2N(M_E + M_I + 1) \geq 3N + M_E + 2M_I + 1 \quad (8)$$

where for the case of equality applied there would likely be ambiguities. If we rearrange the above equation assuming that  $M_E + M_I > 0$  we obtain:

$$N \geq \frac{M_E + 2M_I + 1}{2M_E + 2M_I - 1} \quad (9)$$

From this form we see that the lower bound on  $N$  is 3 only in the case of  $M_E = 0$  and  $M_I = 1$ . In other cases the lower bound is either 1 or 2 (taking into account that  $N$  is an integer). Thus at least 1, 2 or 3 different  $B$  decays must be observed depending (according to eqn. (9)) on how many different  $D$  decays are considered assuming, in all cases, that we observe the CPES- decays of the  $\mathbf{D}^0$ .

As an illustration of this let us assume that the three inclusive modes  $B^- \rightarrow \mathbf{D}^0 K^- \pi^0$ ,  $B^- \rightarrow \mathbf{D}^{*0} K^- \pi^0$  and  $B^- \rightarrow \mathbf{D}^0 K^{*-} \pi^0$  are observed with  $\mathbf{D}^0 \rightarrow CPES-$ ,  $K^+ \pi^-$  and  $K^{*+} \pi^-$  so that  $N = 3$ ,  $M_E = 2$  and  $M_I = 0$ . Clearly Eqn. (8) is satisfied since there are 18 observables for 12 unknowns. To carry out our calculation we will assume that  $a(D^{(*)0} K^{(*)-} \pi^0) = a(D^{(*)0} K^{(*)-})$  and  $b(\bar{D}^{(*)0} K^{*-} \pi^0) = 9b(\bar{D}^{(*)0} K^{*-})$  since it is not color suppressed; also we take  $R = 0.5$  in each case. The results are shown with the dashed line in Fig. 11.

## IX. PROSPECTS FOR $\gamma$ AT A SUPER-B FACTORY

Improvements at the existing asymmetric B-factories at KEK and SLAC are expected to allow luminosity increase to around  $10^{35} cm^{-2} sec^{-1}$ . Further increase in luminosity to  $10^{36} cm^{-2} sec^{-1}$  and beyond will most likely require a new machine[27]. The asymmetric B-factories at KEK and SLAC have made a rather accurate determination of  $\sin(2\beta)$  and established that the CKM-phase is the dominant contributor to the observed CP asymmetry in  $B \rightarrow \psi K_s$ , which has to be regarded an important milestone in our understanding of CP violation phenomena. There is now considerable interest at the construction of an asymmetric ‘‘Super-B Factory’’ (SBF) with luminosity  $10^{36} cm^{-2} sec^{-1}$  or more[28, 29]. Precision determinations of all the angles of the unitarity triangle, roughly in the range of the intrinsic theory error for each of the three angles, and the search for beyond the SM source(s) of CP violation, which are bound to exist, constitute important motivations for such an effort.

In particular,  $\gamma$  can be determined very cleanly from direct CP violation via the generic  $B \rightarrow K^{(*)}D^{0(*)}$  processes. There are multitude of available strategies and modes; several of them we dealt in this paper. Using Fig 2 as a guide we can anticipate possible determination of  $\gamma$  at a Super-B factory with a  $3\text{-}\sigma$  error of a few ( $\approx 2$ ) degrees.

Admittedly backgrounds could make things difficult in an actual experimental setup, as Fig 5 indicates; from the figure we see that the accuracy in determination of  $\gamma$  from these methods may, due to backgrounds, get degraded to  $\approx 7^\circ$  at the Super-B Factory. It should be noted though that strategies used in Fig 2 and Fig 5 are far from exhaustive. For example, one promising technique which we had suggested earlier [5, 6] is Dalitz plot study of 3-body decays of  $D^0$ . Since some experimental data had existed at that time for  $D^0 \rightarrow K^+\pi^-\pi^0$  from Fermilab experiment E687 [30], we had used that specific mode to illustrate the method. More recently CLEO collaboration[31] has also studied  $D^0 \rightarrow K_s\pi^+\pi^-$  which is another interesting candidate where the analysis [6] could be readily applied to extract  $\gamma$ . Indeed preliminary studies of this mode by the BELLE collaboration [32] are quite encouraging.

In addition to Dalitz plot studies of  $D^0$  decays, charm factory running on  $\psi(3770)$  could be very helpful in determination of  $\gamma$  from  $B \rightarrow KD$  approaches as Fig 4 illustrates; see also section VIII and [7].

## X. SUMMARY AND OUTLOOK

In this paper we have extended our previous studies[5, 6, 7] on extraction of  $\gamma$  using direct CP violation in  $B \rightarrow KD$  processes. In principle, these methods are theoretically very clean. The irreducible theory error originating from higher-order weak interactions is  $O(10^{-3})$ [26], i.e. in all likelihood even smaller than the theory error in deducing the angle  $\beta$  using time dependent CP asymmetry in  $B \rightarrow \psi K_s$ . However,  $\gamma$  determination from  $B \rightarrow KD$  is much harder than  $\beta$  from  $B \rightarrow \psi K_s$ .

This study strongly suggests that the demands on machine luminosity can be significantly alleviated if a combination of strategies is used. One interesting handle that we examined here which looks rather promising is to include  $D^{*0}$  from  $B \rightarrow K^{(*)}D^{*0}$ . The formalism for the use of  $D^0$  decays is identical to  $B \rightarrow K^*D^0$  after  $D^{*0} \rightarrow \pi^0(\gamma) + D^0$ .

Similarly including  $K^*$  (via e.g.  $B^- \rightarrow K^{*-}D^0$ ) along with  $B^- \rightarrow K^-D^0$  is helpful. Also it of course helps a great deal to use both CP eigenstates[4] along with CP non-eigenstates of  $D^0$ , whether they be doubly Cabibbo suppressed[5, 6] or singly Cabibbo suppressed[17].

While flavor tagging of the  $D^0$  and  $\bar{D}^0$  is likely to be a challenge, we emphasized that kinematics and topology of the signal events is quite distinct from that of many of the backgrounds so that semi-leptonic tags may have a chance at least for a relatively imprecise determination of the needed color-suppressed branching ratio. If such a determination could be made, say at super-B factory with an error on the branching ratio of around 10-20%, it could become helpful in  $\gamma$  determination.

Many of the modes relevant for gamma determination should exhibit large direct CP-asymmetries; this is especially so in the case of doubly Cabibbo suppressed modes of  $D^0$ . However, as Tables (VIII,XII,XIII) illustrate CP asymmetries in many other modes are also appreciable. Indeed, at least in the initial stages, it may even be useful to target the search for such large asymmetries.

It is difficult to overemphasize the important role that a charm factory running at  $\psi(3770)$  can play in the extraction of  $\gamma$ . Charm factory can of course help by improving on the mixing parameters of the  $D^0 - \bar{D}^0$  complex. It can also help in determination of the doubly Cabibbo suppressed branching ratios as well as in the needed strong phases. Quantum entanglement in  $\psi \rightarrow D^0\bar{D}^0$  decays can also be exploited to determine the coherence factor and the strong phase for inclusive  $D^0$  decays[7].

Note also that all of these studies of charm physics at the charm factory not only have important application to extraction of  $\gamma$  from direct CP studies in  $B \rightarrow KD$  processes, precisely the same information on D-decays and D-mixing can also be used in time dependent CP studies in  $B^0 \rightarrow K^0D^{0(*)}$ ; in that case one gets the linear combination of unitarity angles  $\delta \equiv (2\beta + \gamma) \equiv (\beta - \alpha + \pi)$  and furthermore that method also gives  $\beta$ [12, 14] providing an additional test of the CKM-paradigm.

While B-factories with about  $10^9$  B-pairs are likely to be able to make appreciable progress in determination of  $\gamma$ , super-B factory with luminosity  $\geq 10^{10}$  B-pairs will be needed to extract  $\gamma$  with an accuracy roughly commensurate with the intrinsic theory error that these methods allow. This in itself should constitute an important goal of B-physics in general and super-B factory in particular.

## XI. ACKNOWLEDGMENTS

We would like to thank Tom Browder, Riccardo Faccini, Tim Gershon, Masashi Hazumi, Gerald Raven, Abi Soffer, Sheldon Stone and Sanjay Swain. This research was supported by Contract Nos. DE-FG02-94ER40817 and DE-AC02-98CH10886.

### Appendix: Formalism

Let us now present a summary of the formalism for determining the rates for  $B^- \rightarrow K^{(*)-}[D^{(*)0} \rightarrow F]$  and related processes. Here we will discuss the rates in four situations:

1.  $F$  is an exclusive state; without  $D^0 \bar{D}^0$  oscillations.
2.  $F$  is an inclusive set of states; without  $D^0 \bar{D}^0$  oscillations.
3.  $F$  is an exclusive state where  $D^0 \bar{D}^0$  oscillations are considered
4.  $F$  is an inclusive state where  $D^0 \bar{D}^0$  oscillations are considered.

For this purpose exclusive state refers to a state which is governed by a single quantum amplitude, for instance  $D^0 \rightarrow K^+ \pi^-$ . In contrast an inclusive state is composed of a decay where there are a number of amplitudes contributing incoherently. Some examples are inclusive states made of states with different particle content, for instance  $K^+ + n\pi$  or multibody final states integrated over phase space, for instance  $K^+ \pi^+ \pi^0$  integrated over the Dalitz plot. Note that each point in the  $K^+ \pi^- \pi^0$  Dalitz plot is an exclusive state.

First let us take  $f$  to be an exclusive state. Let us denote by  $d$  the branching ratio for  $B^- \rightarrow K^{(*)-}[D^{(*)0} \rightarrow f]$  where  $D^0$  means a general mixture of  $D^0$  and  $\bar{D}^0$  and  $\bar{d}$  the charge conjugate branching ratio for  $B^+ \rightarrow K^{(*)+}[D^{(*)0} \rightarrow \bar{f}]$ .

For this decay let  $a$  be the branching ratio for  $B^- \rightarrow K^- D^0$  and  $b$  be the branching ratio for  $B^- \rightarrow K^- \bar{D}^0$ . Likewise let us denote by  $c$  the branching ratio for  $D^0 \rightarrow f$  and  $\bar{c}$  the branching ratio for  $\bar{D}^0 \rightarrow f$ . Assuming that  $D^0$  mixing is negligible[5, 6],

$$\begin{aligned} d &= ac_f + b\bar{c}_f + 2\sqrt{abc_f\bar{c}_f} \cos(\zeta_B + \zeta_f + \gamma) \\ \bar{d} &= ac_f + b\bar{c}_f + 2\sqrt{abc_f\bar{c}_f} \cos(\zeta_B + \zeta_f - \gamma) \end{aligned} \quad (10)$$

where  $\zeta_B$  is the strong phase difference between  $B^- \rightarrow K^{(*)-} D^{(*)0}$  and  $B^- \rightarrow K^{(*)-} \bar{D}^{(*)0}$  and  $\zeta_f$  the strong phase difference between  $D^0 \rightarrow f$  and  $\bar{D}^0 \rightarrow \bar{f}$ .

Let us now consider the generalization to the case where  $F$  is an inclusive state,  $F = \{f_1, \dots, f_n\}$  and denote:

$$R_F e^{i\zeta_F} = \frac{\sum_i \sqrt{c_{f_i} \bar{c}_{f_i}} e^{i\zeta_{f_i}}}{\sqrt{c_F \bar{c}_F}} \quad (11)$$

where  $c_F = \sum_i c_{f_i}$  and similarly  $\bar{c}_F$ . For the decay to an inclusive final state  $F$ , then, we can generalize eqn. (10) to:

$$\begin{aligned} d &= ac_F + b\bar{c}_F \\ &\quad + 2R_F \sqrt{abc_F \bar{c}_F} \cos(\zeta_B + \zeta_F + \gamma) \\ \bar{d} &= ac_F + b\bar{c}_F \\ &\quad + 2R_F \sqrt{abc_F \bar{c}_F} \cos(\zeta_B + \zeta_F - \gamma) \end{aligned} \quad (12)$$

Note that in the case where  $F$  is an exclusive state  $R_F = 1$ .

Another, related generalization is the case where the initial  $B^-$  decays to an inclusive state. For instance this is the case in  $B^- \rightarrow K^{*-} D^{*0}$  because there are three helicity amplitudes. Of course the amplitudes may be separated through the consideration of angular distributions in the vector decays. Another instance is a three body decay such as  $B^- \rightarrow K \pi D^0$ .

In general, we can consider  $B^- \rightarrow G$  where  $G$  is an inclusive set of states. Thus, each  $g_i$  contains one (generic)  $D^0$  meson. We will use  $g'_i$  to denote, specifically, the version of the state where the neutral  $D$  is in a  $|D^0\rangle$  state and  $g''_i$  to be the case where the neutral  $D$  is in a  $|\bar{D}^0\rangle$  state. Let us denote the branching ratios  $B^- \rightarrow g'_i$  by  $a_{g_i}$  and  $B^- \rightarrow g''_i$  by  $b_{g_i}$ . One could, in principle, determine  $a_{g_i}$  and  $b_{g_i}$  by observing the semileptonic decay of the  $D^0$ .

Thus, in analogy to Eqn. (11) let us define:

$$R_G e^{i\zeta_G} = \frac{\sum_i \sqrt{a_{g_i} \bar{b}_{g_i}} e^{i\zeta_{g_i}}}{\sqrt{a_{g_i} \bar{b}_{g_i}}} \quad (13)$$

If the neutral  $D$  in  $G$  subsequently decays to an inclusive state  $F$ , then the combined branching ratio is:

$$\begin{aligned} d &= a_G c_F + b_G \bar{c}_F \\ &\quad + 2R_F R_G \sqrt{a_G b_G c_F \bar{c}_F} \cos(\zeta_G + \zeta_F + \gamma) \\ \bar{d} &= a_G c_F + b_G \bar{c}_F \\ &\quad + 2R_F R_G \sqrt{a_G b_G c_F \bar{c}_F} \cos(\zeta_G + \zeta_F - \gamma) \end{aligned} \quad (14)$$

Let us now consider the case where  $D^0 \bar{D}^0$  mixing is present.

First, let us consider the fully general case where, following the usual formalism [6, 33], the eigenstates of neutral  $D$  meson are:

$$\begin{aligned} |D_1\rangle &= p|D^0\rangle + q|\bar{D}^0\rangle \\ |D_2\rangle &= p|D^0\rangle - q|\bar{D}^0\rangle \end{aligned} \quad (15)$$

with corresponding masses  $m_1, m_2$  and widths  $\Gamma_1, \Gamma_2$ . These are characterized by the parameters:

$$x = \frac{m_2 - m_1}{\Gamma}, \quad y = \frac{\Gamma_2 - \Gamma_1}{2\Gamma} \quad (16)$$

where  $2\Gamma = \Gamma_1 + \Gamma_2$ .

If  $p/q \neq 1$  then CP is violated in the mixing. If this is indeed the case, one would expect that there would also be CP violating phases in the decay. In the following we will assume that  $D$  decays are CP conserving and then indicate how to generalize to the case of CP violation in the final state. In this case the decay amplitudes of  $D^0$  only have strong phases and we denote:

$$\frac{p}{q} = \exp^{A+i\phi} \quad (17)$$

Thus, generalizing Eqn. (14) to the case where there is  $D^0$  mixing and integrating over time:

$$\begin{aligned} d &= \frac{Q+P}{2} \left[ a_G c_F + b_G \bar{c}_F \right. \\ &\quad \left. + 2R_F R_G \sqrt{a_G c_F b_G \bar{c}_F} \cos(\eta_G + \gamma + \eta_F) \right] \\ &+ \frac{Q-P}{2} \left[ e^{2A} a_G c_F + e^{-2A} b_G \bar{c}_F \right. \\ &\quad \left. + 2R_F R_G \sqrt{a_G c_F b_G \bar{c}_F} \cos(\eta_G + \gamma - \eta_F) \right] \\ &- yQ \left[ c_F \sqrt{a_G b_G} R_G e^A \cos(\eta_G + \gamma + \phi) \right. \\ &\quad + \bar{c}_F \sqrt{a_G b_G} R_G e^{-A} \cos(\eta_G + \gamma - \phi) \\ &\quad + a_G \sqrt{c_F \bar{c}_F} e^{-A} R_F \cos(\eta_F + \phi) \\ &\quad \left. + b_G \sqrt{c_F \bar{c}_F} e^A R_F \cos(\eta_F - \phi) \right] \\ &+ xP \left[ c_F \sqrt{a_G b_G} R_G e^A \sin(\eta_G + \gamma + \phi) \right. \\ &\quad + \bar{c}_F \sqrt{a_G b_G} R_G e^{-A} \sin(\eta_G + \gamma - \phi) \\ &\quad + a_G \sqrt{c_F \bar{c}_F} e^{-A} R_F \sin(\eta_F + \phi) \\ &\quad \left. + b_G \sqrt{c_F \bar{c}_F} e^A R_F \sin(\eta_F - \phi) \right] \end{aligned} \quad (7)$$

$$\begin{aligned}
\bar{d} = & \frac{Q+P}{2} \left[ a_G c_F + b_G \bar{c}_F \right. \\
& \left. + 2R_F R_G \sqrt{a_G c_F b_G \bar{c}_F} \cos(\eta_G - \gamma + \eta_F) \right] \\
& + \frac{Q-P}{2} \left[ e^{-2A} a_G c_F + e^{2A} b_G \bar{c}_F \right. \\
& \left. + 2R_F R_G \sqrt{a_G c_F b_G \bar{c}_F} \cos(\eta_G - \gamma - \eta_F) \right] \\
& - yQ \left[ c_F \sqrt{a_G b_G} R_G e^{-A} \cos(\eta_G - \gamma - \phi) \right. \\
& + \bar{c}_F \sqrt{a_G b_G} R_G e^A \cos(\eta_G - \gamma + \phi) \\
& + a_G \sqrt{c_F \bar{c}_F} e^A R_F \cos(\eta_F - \phi) \\
& \left. + b_G \sqrt{c_F \bar{c}_F} e^{-A} R_F \cos(\eta_F + \phi) \right] \\
& + xP \left[ c_F \sqrt{a_G b_G} R_G e^{-A} \sin(\eta_G - \gamma - \phi) \right. \\
& + \bar{c}_F \sqrt{a_G b_G} R_G e^A \sin(\eta_G - \gamma + \phi) \\
& + a_G \sqrt{c_F \bar{c}_F} e^A R_F \sin(\eta_F - \phi) \\
& \left. + b_G \sqrt{c_F \bar{c}_F} e^{-A} R_F \sin(\eta_F + \phi) \right] \tag{-3}
\end{aligned}$$

where

$$P = \frac{1}{1+x^2}, \quad Q = \frac{1}{1-y^2} \tag{-2}$$

Note that in the limit that  $x, y, A, \phi \rightarrow 0$  these equations reduce to Eqn. (14).

- 
- [1] N. Cabibbo, Phys. Rev. Lett. **10**, 531 (1963); M. Kobayashi and T. Maskawa, Prog. Th. Phys. **49**, 652 (1973).  
[2] K. Abe et al (BABAR Collab), Phys. Rev. D **66**, 071102 (2002)  
[3] B. Aubert et al (BABAR Collab), Phys. Rev. Lett. **89**, 201802 (2002).  
[4] M. Gronau and D. Wyler, Phys. Lett. **B265** (1991); M. Gronau and D. London., Phys. Lett. **B253**, 483 (1991).  
[5] D. Atwood, I. Dunietz and A. Soni, Phys. Rev. Lett. **78**, 3257 (1997).  
[6] D. Atwood, I. Dunietz and A. Soni, Phys. Rev. D **63**, 036005 (2001).  
[7] D. Atwood and A. Soni, arXiv:hep-ph/0304085.  
[8] D. London, N. Sinha and R. Sinha, arXiv:hep-ph/0304230; Phys. Rev. Lett. **85**, 1807 (2000).  
[9] N. Deshpande and A. Soni, Snowmass Proceedings 1986, p.58 (Eds. R. Donaldson and J. Marx).  
[10] I. Dunietz, Phys. Lett. B **270**, 75 (1991).  
[11] G. Branco, L. Lavoura, J. Silva in *CP Violation*, Oxford Univ. Press (1999), esp. p.445.  
[12] B. Kayser and D. London, Phys. Rev. D **61**, 116013 (2000).  
[13] A.I. Sanda, hep-ph/0108031.  
[14] D. Atwood and A. Soni, arXiv:hep-ph/0206045.  
[15] R. Fleischer, Nucl. Phys. B659 (2003), 321; Phys. Lett. B 562, 234(2003).  
[16] R. Aleksan, T. C. Petersen and A. Soffer, Phys. Rev. D **67**, 096002 (2003).  
[17] Y. Grossman, Z. Ligeti and A. Soffer, hep-ph/0210433;  
[18] K. Hagiwara *et al.* [Particle Data Group Collaboration], Phys. Rev. D **66**, 010001 (2002).  
[19] Soren Prell, private communication.

- [20] A. Soffer, arXiv:hep-ex/9801018.
- [21] J. P. Silva and A. Soffer, Phys. Rev. D **61**, 112001 (2000).
- [22] M. Gronau, Y. Grossman and J. L. Rosner, Phys. Lett. B **508**, 37 (2001).
- [23] A. Giri, Y. Grossman, A. Soffer and J. Zupan, arXiv:hep-ph/0303187.
- [24] See, e.g. Atwood and Soni, Phys. Lett. B508, 17 (2001)
- [25] M. Gronau, Phys. Rev. Lett. **83**, 4005 (1999).
- [26] D. Atwood and A. Soni, hep-ph/0212071
- [27] See the talk by Masa Yamamuchi (BELLE) at the 5th Workshop on Higher Luminosity B-FactorY (Sept 24-26,2003), Izu, Japan.
- [28] See the Proceedings of 5th Workshop on Higher Luminosity B-FactorY (Sept 24-26,2003), Izu, Japan: *http : //belle.kek.jp/superb/workshop/2003/HL05/program.htm*
- [29] See the Proceedings of the Second Workshop on the Discovery Potential of an Asymmetric B-FactorY at  $10^{36}$  Luminosity (Oct 22-24,2003), SLAC: *http:// www.slac.stanford.edu/ BFROOT/www/ Organization/ 1036\_Study\_Group/ 0310Workshop/*
- [30] P. L. Frabetti *et al.* [E687 Collaboration], Phys. Lett. B **331**, 217 (1994).
- [31] H. Muramatsu *et al.* (CLEO), Phys. Rev. Lett. **89**,251802,2002; Erratum-ibid 90,059901,2003.
- [32] K. Abe *et al.* (BELLE), hep-ex/0308043.
- [33] See, e.g. Z. Xing, Phys. Rev. **D55**, 196(1997); T. Liu *Tau Charm Factory Workshop, Argonne IL (1995)*.